Chance Constrained Reserve Scheduling Using Uncertain Controllable Loads Part I: Formulation and Scenario-Based Analysis

Maria Vrakopoulou, *Member, IEEE*, Bowen Li, *Student Member, IEEE*, and Johanna L. Mathieu, *Member, IEEE*

***Abstract*—This paper develops a multi-period chance constrained optimal power flow model to schedule generation and reserves from both generators and aggregations of controllable electric loads. In contrast to generator-based reserve capacities, load-based reserve capacities are less certain because they depend on load usage patterns and ambient conditions. This paper is divided in two parts. In part I, we develop a reserve scheduling framework managing uncertain power from wind and uncertain reserves provided by controllable loads, and solve the problem using a probabilistically robust optimization method that may require large numbers of uncertainty scenarios but provides *a priori* guarantees on the probability of constraint satisfaction, assuming no knowledge of the uncertainty distributions. The solution of this problem offers us a policy-based strategy for real-time reserve deployment. We derive simple rules, based on the cost parameters of the resources, to determine when load-based reserves will be preferable. In part II, we reformulate the problem assuming the uncertainty follows multivariate normal distributions and re-solve the problem, comparing the results against the randomized technique. To evaluate the performance of the methods, we conduct simulations using the IEEE 30-bus network.**

***Index Terms*—Chance constrained optimization, load control, multi-period optimal power flow, reserve policies, probabilistically robust optimization, wind power integration.**

I. Introduction

As THE grid penetration of fluctuating renewable energy sources increases, more reserves are needed to balance supply and demand. Thermal and hydropower plants typically provide balancing reserves to power systems, but aggregations of electric loads may be able to do so at lower cost and/or with less environmental impact [1]. Recent studies have developed methods to use commercial and residential loads to provide balancing reserves such as load following and frequency regulation, e.g., [2] and [3]. Loads are coordinated to decrease and increase their consumption with respect to their baseline consumption to provide up and down balancing. Recent studies have also developed methods to dispatch controllable loads within the optimal power flow or unit commitment problem [4], [5].

To manage power system uncertainty stemming from fluctuating renewable power production and loads, we can formulate and solve stochastic optimal power flow problems. One method is to minimize the expected cost of operating the power system over a heuristically-chosen finite number of uncertainty scenarios, e.g., [6]. Another method is to formulate a chance constrained optimization problem in which constraints with random variables hold probabilistically, ensuring feasibility for a vast majority of uncertainty scenarios, see [7], [8]. In [9] a chance constrained formulation to schedule the production levels and reserve capacities for generators in systems with uncertain renewable energy production is proposed. It is straightforward to extend this approach to additionally schedule the reserve capacities of aggregations of controllable loads if we assume the available reserve capacity is known. However, in practice, the available reserve capacity of an aggregation of loads is a function of random variables such as ambient conditions (e.g., the capacity of an aggregation of air conditioners is a function of outdoor temperature) and load usage patterns (e.g., the capacity of an aggregation of electric vehicles is a function of driving patterns) [10].

The main objective of this two-part paper is to design and analyze a chance-constrained optimal power flow (CC-OPF) formulation to schedule generator production and load consumption levels along with both generator and load-based reserve capacities assuming uncertainty in renewable energy production and the available reserve capacity of the controllable loads. We model controllable loads as thermal energy storage units and design a redispatch[1] mechanism to manage the energy state (comparable to a battery's state of charge) of the loads to minimize uncertainty propagation throughout the time horizon. We consider uncertainty in both wind forecasts and outdoor temperature forecasts, where the latter affects the available capacity from controllable loads.

Manuscript received March 19, 2017; revised July 5, 2017 and September 27, 2017; accepted November 9, 2017. Date of publication November 15, 2017; date of current version February 18, 2019. This work was supported by the European Commission through the Project SOPRIS under Grant PIOF-GA-2013-626014, and in part by the U.S. NSF under Grant CCF-1442495. Paper no. TSG-00384-2017. *(Corresponding author: Johanna L. Mathieu.)*

M. Vrakopoulou is with the Automatic Control Laboratory, ETH Zurich, 8092 Zurich, Switzerland (e-mail: vrakopoulou@control.ee.ethz.ch).

B. Li and J. L. Mathieu are with the Department of Electrical Engineering and Computer Science, University of Michigan, Ann Arbor, MI 48109 USA (e-mail: libowen@umich.edu; jlmath@umich.edu).

Color versions of one or more of the figures in this paper are available online at http://ieeexplore.ieee.org.

Digital Object Identifier 10.1109/TSG.2017.2773627

[1]Note that, in Europe, the term "redispatch" is used differently, i.e., to describe the adjustment of generator active powers so as to alleviate potential transmission or N–1 security constraint violations.

In Part I, we develop the formulation and solve the problem using a probabilistically robust optimization method [11], [12] that may require large numbers of uncertainty scenarios, but provides a priori guarantees on the probability of constraint violation, assuming no knowledge of the uncertainty distributions. In Part II, we reformulate the problem assuming the uncertainty follows multivariate normal distributions and resolve the problem, comparing the results against those of the scenario-based method. Other recent studies also solve CC-OPF problems using the same scenario-based method [8], [9] or via analytical reformulation, e.g., [13] and [14], but these studies do not model load-based reserves or their uncertainty. Reference [15] formulates a simpler, single-period CC-OPF with uncertain renewable energy production and load-based reserve capacities. In contrast, our multi-period formulation leads to lower-cost, higher-reliability solutions because it manages uncertainties jointly throughout a 24-hour horizon. Like most of the related work [8], [9], [13]–[15], we use the DC power flow approximation for simplicity, though our formulation could be extended to include the AC power flow equations and solved using recently developed methods [16], [17].

The contributions compared to our preliminary work [18], [19] are as follows. 1) We modify the CC-OPF formulation to more accurately model the energy state dynamics of the controllable loads (Part I). 2) We redesign the controllable load model to more accurately model deviations due to temperature forecast error (Part I). 3) We derive relations between the reserve dispatch and the reserve costs, which determine when load-based reserves will be preferred over generator reserves (Part I). 4) We model uncertainty using correlated multivariate distributions and provide analytical reformulations for the full realistic range of temperature forecasts (Part II). 5) We show that the analytical reformulation is convex (Part II). Both parts explore a wider range of case studies than [18], [19].

Part I is organized as follows. Section II describes the model, Section III introduces the formulation of the CC-OPF, and Section IV describes the solution methodology. Section V introduces simple cost parameter rules that determine the least-expensive reserve resource and Section VI presents the results of case studies on the IEEE 30-bus network. Concluding remarks are provided in Section VII.

II. Modelling

A. Uncertain Controllable Loads

In this work, we assume that aggregations of thermostatically controlled loads (TCLs) comprise a portion of the total system load. Each TCL is locally controlled to maintain its internal temperature within a narrow temperature range (e.g., 1°C) by switching on/off its power consumption. Because they operate within a temperature range, TCLs have inherent flexibility, i.e., we can coordinate their switching to shift their consumption in time (ensuring that the total amount of energy delivered over a specific longer time horizon is fixed) without violating their temperature constraints.

We can model the aggregations of TCLs as thermal energy storage units [20]. We assume that the aggregator is able to broadcast control signals to all TCLs inducing on/off switching actions achieving a desired aggregate power consumption $P_{C,t}$. When the ambient conditions are constant, the energy state S_t of the aggregation evolves with time steps t of length $\Delta\tau$ as

$$S_{t+1} = S_t + \big(P_{C,t} - P_{B,t}\big)\Delta\tau, \tag{1}$$

where $P_{B,t}$ is the baseline aggregate power consumption, i.e., the consumption that would have occurred without external scheduling. Actions which decrease (increase) consumption relative to the baseline empty (charge) the storage unit.

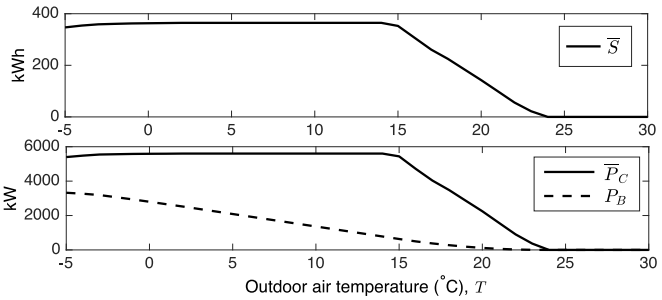

Fig. 1. Energy capacity, power capacity, and baseline power consumption of an aggregation of electric heaters modeled as a thermal energy storage unit.

A TCL aggregation's baseline consumption, power capacity (i.e., limits for $P_{C,t}$), and energy capacity (i.e., limits for S_t) are a function of a variety of time-dependent uncertain quantities such as ambient conditions and load usage patterns. Here, we assume outdoor air temperature T_t alone determines the baseline consumption $P_B(T_t)$, the power capacity $\overline{P}_C(T_t)$, and the energy capacity $\overline{S}(T_t)$, i.e.,

$$0 \le P_{C,t} \le \overline{P}_C(T_t), \quad 0 \le S_t \le \overline{S}(T_t).$$

In [20], a method of computing $P_B(T_t)$, $\overline{P}_C(T_t)$, and $\overline{S}(T_t)$ for an aggregation of residential electric space heaters or air conditioners is described. Here, we use this method to compute these quantities for an aggregation of 1,000 heterogenous electric space heaters. Specifically, individual heaters are modeled using the hybrid model first developed in [21] and [22] and commonly used in load control research, e.g., [23]. We use the heterogeneous heat pump parameters (including temperature set points, thermal capacitances, thermal resistances, etc.) from [24], which were tuned using real data. Applying the equations from [20], we obtain the results shown in Fig. 1. We assume that the values in Fig. 1 are accurate for a given outdoor air temperature but that our forecasts of outdoor air temperature are uncertain. Hence Fig. 1 serves as a look-up table which maps an outdoor air temperature forecast to the baseline consumption, power capacity, and energy capacity of a thermal energy storage unit. We neglect uncertainty stemming from consumer interaction with the heaters, e.g., choosing to switch off heaters even when the indoor temperature is below the temperature set point. The formulation could be easily extended to include additional uncertainties affecting the aggregate load power/energy capacities. Furthermore, thermal energy storage model error could be treated as uncertainty and included in the formulation.

When ambient conditions are changing, the energy state equation (1) must be modified to take into account changes in the energy capacity. Specifically, for heating loads, when T_t increases, $\overline{S}$ may decrease (as shown in Fig. 1) because T_{t+1} is within or above some heaters' temperature range and those heaters are no longer available for control. We can assume that the aggregation of heaters that become unavailable in $t+1$ had approximately the same percent energy state $S_t/\overline{S}(T_t)$ as the aggregation of all heaters available in t. Therefore, when T_t increases, we assume the percent energy state at the beginning of time-step $t+1$ is the same as the percent energy state at the end of time step t. When T_t decreases, $\overline{S}(T_t)$ may increase because heaters that were previously unavailable become available. We assume that the heaters that become available have a 50% energy state. With these assumptions, the new energy state equation is

$$S_{t+1} = \big(S_t + (P_{C,t} - P_B(T_t))\Delta\tau\big)\min\left(\frac{\overline{S}(T_{t+1})}{\overline{S}(T_t)}, 1\right) + 0.5\max\big(\overline{S}(T_{t+1}) - \overline{S}(T_t), 0\big). \quad (2)$$

Note that, while we focus on TCLs within this work because TCL aggregations are well-suited to providing reserves and their power/energy capacities are uncertain, our formulation could be easily extended to accommodate any energy-constrained load/storage aggregation with power/energy capacity uncertainty. Ultimately any type of load/storage aggregation or aggregations of diverse loads/storage can be approximately modeled with (1), as demonstrated by a variety of recent work, e.g., [10] and [25]–[28]. Generally an aggregation's power/energy capacity will be uncertain because of disturbances and model error. For example, [25] develops a method to approximate the power/energy capacity of aggregations of electric vehicles; however, these capacities will be uncertain because of disturbances (e.g., consumers connecting/disconnecting their electric vehicles at different times than forecasted) and model error (i.e., the full set of battery dynamics/constraints are not represented by the aggregate model) [10].

B. Generation-Load Mismatch

We consider two types of uncertainty: uncertainty on the wind power forecast and uncertainty on the outdoor temperature forecast. If the system is operated based on the forecasts, forecast error may create generation-load mismatch, which should be compensated by reserves to maintain power balance. When the controllable loads are unscheduled, they consume the baseline power and hence the total generation-load mismatch is the sum of the total wind power forecast error and the total baseline power forecast error, i.e.,

$$P_{m,t} = \mathbf{1}^T\Big(P_{W,t} - P^f_{W,t}\Big) + \mathbf{1}^T\Big(P_B(T_t) - P_B\Big(T^f_t\Big)\Big), \quad (3)$$

where $P_{W,t}$ and $P^f_{W,t}$ are vectors including the actual and forecast wind power production of each wind power plant, respectively. Similarly, $P_B(T_t)$ and $P_B(T^f_t)$ are vectors including the actual and forecast baseline power consumption of each controllable load aggregation, respectively. The vector $\mathbf{1}$ is a unit vector with the same dimension as the vector that it is multiplied with, and so $P_{m,t}$ is a scalar.

When the controllable loads are scheduled, their consumption is no longer uncertain and hence the generation-load mismatch is only the total wind power forecast error, i.e.,

$$P_{m,t} = \mathbf{1}^T\Big(P_{W,t} - P^f_{W,t}\Big). \quad (4)$$

In this case, as detailed later, both types of uncertainty will affect the energy state trajectory.

C. Reserve Policies

We assume that secondary frequency control (i.e., automatic generation control) compensates power mismatches on the timescale of seconds to minutes and tertiary frequency control is activated periodically to redispatch the system. We refer to the former as "secondary reserves" and the latter as "redispatch reserves," which are comparable to real-time energy market actions in the U.S. Traditionally, reserve capacities are determined via heuristic rules, for example, as a function of load and renewable energy production forecasts, and are *inputs* to the OPF. Reference [29] proposes an advanced dynamic probabilistic reserve sizing method that uses nonparametric forecast error distributions to determine required reserve capacities. In contrast, minimum-cost adequate capacities of secondary and redispatch reserves are *outputs* of our CC-OPF. We assume both generators and controllable loads can provide secondary reserves, but only generators provide redispatch reserves.

To determine the adequate secondary or redispatch reserve capacity, we need to model the operating point after a control action. In [8] the new generation set point P^{new}_G is modeled using an affine function of the power mismatch while [30] differentiates between positive and negative generation-load mismatch by using a piecewise affine function. Following [18], we model P^{new}_G and the new controllable load set point P^{new}_C using piecewise affine functions, which gives us the policies

$$P^{new}_{G,t} = P_{G,t} + \overline{d}_{G,t}\max\big(-P_{m,t}, 0\big) - \underline{d}_{G,t}\max\big(P_{m,t}, 0\big), \quad (5)$$

$$P^{new}_{C,t} = P_{C,t} + \overline{d}_{L,t}\max\big(P_{m,t}, 0\big) - \underline{d}_{L,t}\max\big(-P_{m,t}, 0\big), \quad (6)$$

where $P_{G,t}$ and $P_{C,t}$ denote the generator and controllable load set points that maintain power balance for the forecasts $P^f_{W,t}$ and T^f_t. To achieve power balance under forecast error, a positive mismatch decreases the power production of generators and increases the power consumption of controllable loads as a function of the distribution vectors $d \geq 0$, where $\mathbf{1}^T\overline{d}_{G,t} + \mathbf{1}^T\underline{d}_{L,t} = 1$ and $\mathbf{1}^T\underline{d}_{G,t} + \mathbf{1}^T\overline{d}_{L,t} = 1$, and each d is treated as a decision variable. Adequate reserve capacities are determined by the amount that the generators (controllable loads) may need to increase/decrease their production (consumption) as a function of $P_{m,t}$. The exact constraints used within the optimization problem are defined in Section III; for notational simplicity we define

$$f(d_1, d_2, x) = d_1\max(-x, 0) - d_2\max(x, 0). \quad (7)$$

D. Market Setup

Our multi-period OPF dispatches resources hourly over a 24-hour horizon, where $\Delta\tau = 1$ hour. Generator and controllable load set points and all reserve capacities are constant within each hour. Secondary reserve may be activated at any point within the hour but redispatch is activated every $\Delta\tau/n$ minutes, where n is the number of intra-hour redispatch intervals. Here, we use $\Delta\tau/n = 5$, 10, or 15 minutes. Redispatch compensates not only the generation-load mismatch but also unforecasted deviations in the energy state of the controllable loads, similar to the California Independent System Operator's Regulation Energy Management functionality [31]. Forecasted changes in the load energy state result from differences between $P_{C,t}$ and $P_B(T_t^f)$, as shown in (1). Unforecasted changes result from load-based secondary reserve actions used to compensate wind power forecast error and baseline error resulting from temperature forecast error. Hence, the actual change in load energy state in each time step will be $(P_{C,t}+R_t-P_B(T_t))\Delta\tau$, where R_t is the reserve action. When the system is redispatched, generator production and controllable load consumption are adjusted to compensate for unforecasted changes in the load energy state over the previous $\Delta\tau/n$ minutes. This ensures that the actual load energy state trajectory is closer to the forecasted one, and increases the ability of the controllable loads to continue providing reserves.

We assume temperature forecast errors, and so baseline power forecast errors, are constant within each hour whereas wind power forecast errors may appear at any time within each hour and may persist until the end of the hour. Fig. 2 shows an example of how three types of forecast error affect reserve actions.

1) Baseline power forecast error causes i) load energy state deviations and ii) generator deviations (via redispatch) and load deviations that stop the increase of these deviations.
2) Wind power forecast error causes i) load and generator deviations (via secondary reserves) to compensate this error, ii) resulting load energy state deviations, and iii) generator deviations (via redispatch) that compensate the wind power forecast error and the load energy state deviations.
3) Remaining load energy state deviations from the previous hour (resulting from baseline power forecast error in the previous hour and/or secondary reserve actions in the last $\Delta\tau/n$-minute interval of the previous hour) cause i) generator deviations (via redispatch) and load deviations that drive the load energy state back to zero, and ii) resulting load energy state deviations.

We show the responses to each of the three errors independently for clarity; in reality all three errors will occur simultaneously and the required generation/load deviations will be the sum of those shown.

Given our assumptions, we only need to check that the system constraints are satisfied at three intra-hour operating points, i.e., if the constraints are satisfied at these points they will be satisfied at all intra-hour operating points.

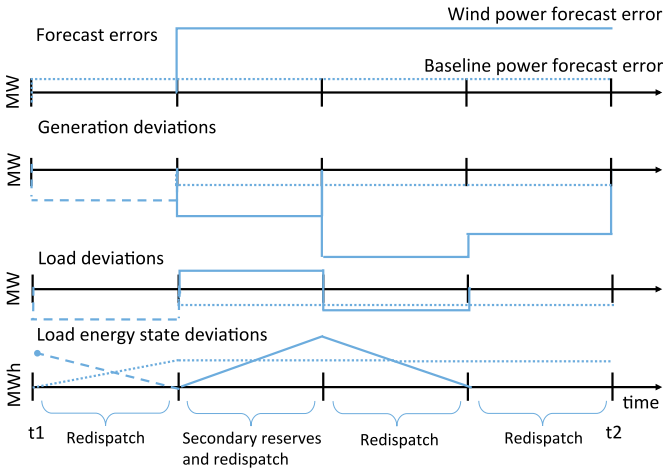

Fig. 2. An example of how forecast errors activate secondary and redispatch reserves and influence the load energy state ($n = 4$). Dotted lines correspond to responses to baseline power forecast error, continuous lines to wind power forecast error, and dashed lines to the remaining load energy state deviation from the previous hour.

Operating Point 1 corresponds to the end of any $\Delta\tau/n$-minute interval, except the first, in which generators provide redispatch to compensate load energy state deviations due to the baseline power forecast error of the previous $\Delta\tau/n$-minute interval and also provide secondary reserve actions. In Fig. 2, this point is reached at the 30^{th} minute.

Operating Point 2 corresponds to the end of any $\Delta\tau/n$-minute interval, except the first, in which generators provide redispatch to compensate the wind power forecast error, load energy state deviations due to baseline power forecast error, and load-based secondary reserve actions of the previous $\Delta\tau/n$-minute interval, but do not provide secondary reserve actions. In Fig. 2, this point is reached at the 45^{th} minute.

Operating Point 3 corresponds to the end of the first $\Delta\tau/n$-minute interval, in which generators provide redispatch to compensate the remaining load energy state deviation from the previous hour and may also provide secondary reserves actions. In Fig. 2, this point is reached at the 15^{th} minute.

III. CC-OPF Formulation

In this section, we present a CC-OPF formulation that co-optimizes energy and reserves provided both by generators and controllable loads under the market setup described in Section II-D taking into account wind power and temperature forecast uncertainty. The objective is to find the generation/controllable load set points (i.e., the dispatch), reserve capacities, and distribution vectors that minimize the energy, secondary reserve, and redispatch costs such that system constraints are satisfied in a probabilistic sense.

A. Notation & Reserve Constraints

We use an optimization horizon $N_t = 24$ hours with hourly steps t. Each load is comprised of an uncontrollable portion $P_{L,t}$, which is assumed known and constant over a time step t, and a controllable portion $P_{C,t}$. For each step t, we define

the vector of decision variables as $x_t = \langle P_t, d_t, \mathcal{R}_t \rangle$, where we use angle brackets to stack column vectors into a single column vector (i.e., $\langle \alpha, \beta \rangle = [\alpha^T, \beta^T]^T$) and P_t contains the generator and load dispatch $\langle P_{G,t}, P_{C,t} \rangle$, d_t the distribution vectors $\langle \underline{d}_{GS,t}, \overline{d}_{GS,t}, \underline{d}_{LS,t}, \overline{d}_{LS,t}, \underline{d}_{GD,t}, \overline{d}_{GD,t} \rangle$ and $\mathcal{R}_t$ the reserve capacities $\langle \underline{R}_{GS,t}, \overline{R}_{GS,t}, \underline{R}_{LS,t}, \overline{R}_{LS,t}, \underline{R}_{GD,t}, \overline{R}_{GD,t} \rangle$. The subscripts *GS*/*LS* correspond to generation/load secondary reserves and *GD* to generation redispatch reserves. Vector $\underline{d}_{GD,t} = \langle \underline{d}^{w}_{GD,t}, \underline{d}^{b}_{GD,t}, \underline{d}^{w_o}_{GD,t}, \underline{d}^{b_o}_{GD,t} \rangle$ and $\overline{d}_{GD,t} = \langle \overline{d}^{w}_{GD,t}, \overline{d}^{b}_{GD,t}, \overline{d}^{w_o}_{GD,t}, \overline{d}^{b_o}_{GD,t} \rangle$, where the component vectors correspond to redispatch actions initiated for different reasons, as described below. We use the subscript *LD* to denote variables related to load adjustments initiated by a redispatch. We denote the baseline power forecast error by $\Delta P_{B,t} = P_B(T_t) - P_B(T^f_t)$ and the total baseline power deviation by $P^b_{m,t} = \mathbf{1}^T \Delta P_{B,t}$. Since we choose $P_{C,t}$ (and the uncontrollable load is assumed known), the generation-load mismatch $P_{m,t}$ is given by (4). We next describe the four types of reserve actions.

1) Secondary Reserves Due to Wind Power Forecast Error: Wind power forecast error activates secondary reserves and $P_{m,t}$ is distributed to generators and controllable loads by shifting their power injection by $R_{GS,t}$ and $R_{LS,t}$, respectively. Using the piecewise linear policy defined in Section II-C, the constraints are

$$R_{GS,t} = f\big(\overline{d}_{GS,t}, \underline{d}_{GS,t}, P_{m,t}\big), \tag{8}$$

$$R_{LS,t} = f\big(\overline{d}_{LS,t}, \underline{d}_{LS,t}, -P_{m,t}\big), \tag{9}$$

$$\mathbf{1}^T \overline{d}_{GS,t} + \mathbf{1}^T \underline{d}_{LS,t} = 1, \tag{10}$$

$$\mathbf{1}^T \underline{d}_{GS,t} + \mathbf{1}^T \overline{d}_{LS,t} = 1. \tag{11}$$

2) Redispatch Compensating Secondary Reserve Actions: After the secondary reserves have achieved power balance, redispatch redistributes the power mismatch $P_{m,t}$ to the generators and compensates unforecasted energy state deviations due to prior load-based secondary reserve actions. Let the power injection shift for the generators be $R^w_{GD,t}$ and for the loads be $R^w_{LD,t}$, which should be of the same magnitude and opposite sign as $R_{LS,t}$. To maintain power balance, the distribution vectors should sum to one plus the portion of the mismatch compensated by the loads. The constraints are

$$R^w_{GD,t} = f\big(\overline{d}^w_{GD,t}, \underline{d}^w_{GD,t}, P_{m,t}\big), \tag{12}$$

$$R^w_{LD,t} = -R_{LS,t}, \tag{13}$$

$$\mathbf{1}^T \overline{d}^w_{GD,t} = 1 + \mathbf{1}^T \underline{d}_{LS,t}, \tag{14}$$

$$\mathbf{1}^T \underline{d}^w_{GD,t} = 1 + \mathbf{1}^T \overline{d}_{LS,t}. \tag{15}$$

3) Redispatch Due to Baseline Power Forecast Error: Baseline power forecast error results in unforecasted energy state deviations, which are compensated by redispatch. Let the power injection shift for the generators be $R^b_{GD,t}$ and for the loads be $R^b_{LD,t}$. The generators should compensate $P^b_{m,t}$, while the loads should shift by $\Delta P_{B,t}$. The constraints are

$$R^b_{GD,t} = f\big(\overline{d}^b_{GD,t}, \underline{d}^b_{GD,t}, -P^b_{m,t}\big), \tag{16}$$

$$R^b_{LD,t} = \Delta P_{B,t}, \tag{17}$$

$$\mathbf{1}^T \overline{d}^b_{GD,t} = 1, \tag{18}$$

$$\mathbf{1}^T \underline{d}^b_{GD,t} = 1. \tag{19}$$

4) Redispatch at the Beginning of an Hour: Redispatch is activated in the first $\Delta\tau/n$-minute interval to compensate energy state deviations from the previous hour $t-1$. The constraints, similar to those above, are

$$R^{w_o}_{GD,t} = f\big(\overline{d}^{w_o}_{GD,t}, \underline{d}^{w_o}_{GD,t}, P_{m,t-1}\big), \tag{20}$$

$$R^{b_o}_{GD,t} = f\big(\overline{d}^{b_o}_{GD,t}, \underline{d}^{b_o}_{GD,t}, -P^b_{m,t-1}\big), \tag{21}$$

$$R^{w_o}_{LD,t} = -R_{LS,t-1} \tag{22}$$

$$R^{b_o}_{LD,t} = \Delta P_{B,t-1} \tag{23}$$

$$\mathbf{1}^T \overline{d}^{w_o}_{GD,t} = \mathbf{1}^T \underline{d}_{LS,t-1}, \tag{24}$$

$$\mathbf{1}^T \underline{d}^{w_o}_{GD,t} = \mathbf{1}^T \overline{d}_{LS,t-1}, \tag{25}$$

$$\mathbf{1}^T \overline{d}^{b_o}_{GD,t} = 1, \tag{26}$$

$$\mathbf{1}^T \underline{d}^{b_o}_{GD,t} = 1. \tag{27}$$

B. Optimization Problem

Let c_1 and c_2 be the generation cost vector and matrix, respectively, and c_R be the reserve cost vector. The optimization problem is

$$\min_{\{x_t\}_{t=1}^{N_t}} \sum_{t=1}^{N_t} \big(P^T_{G,t}[c_2] P_{G,t} + c_1^T P_{G,t} + c_R^T \mathcal{R}_t\big), \tag{28}$$

subject to deterministic constraints and probabilistic constraints corresponding to the three points described in Section II-D, which we describe in the following subsections. All constraints should be satisfied for all $t = 1, \ldots, N_t$.

1) Deterministic Constraints:

$$\mathbf{1}^T P_{inj,t} = 0, \tag{29}$$

$$-P_l \le A P_{inj,t} \le P_l, \tag{30}$$

$$\underline{P}_G \le P_{G,t} \le \overline{P}_G, \tag{31}$$

$$\underline{P}_C\Big(T^f_t\Big) \le P_{C,t} \le \overline{P}_C\Big(T^f_t\Big), \tag{32}$$

$$0 \le S_t \le \overline{S}\Big(T^f_t\Big), \tag{33}$$

$$0 \le S_t + \Big(P_{C,t} - P_B\Big(T^f_t\Big)\Big)\Delta\tau \le \overline{S}\Big(T^f_t\Big), \tag{34}$$

$$S_{t+1} = \Big(S_t + \Big(P_{C,t} - P_B\Big(T^f_t\Big)\Big)\Delta\tau\Big) \min\left(\frac{\overline{S}\Big(T^f_{t+1}\Big)}{\overline{S}\Big(T^f_t\Big)}, 1\right) + 0.5 \max\Big(\overline{S}\Big(T^f_{t+1}\Big) - \overline{S}\Big(T^f_t\Big), 0\Big), \tag{35}$$

$$S_1 = 0.5\overline{S}\Big(T^f_1\Big), \quad S_{N_t+1} = 0.5\overline{S}\Big(T^f_{N_t+1}\Big), \tag{36}$$

where $P_{inj,t} = C_G P_{G,t} + C_W P^f_{W,t} - C_L(P_{L,t} + P_{C,t})$ and the C matrices map the generators, wind power plants, and loads to the buses. Constraint (29) enforces power balance given the wind power forecast; (30), (31), and (32) encode the line, generation, and controllable load capacity limits, respectively, where A is a constant matrix that depends on the network impedances [8]; (33) and (34) ensure that the load energy state is within its limits at the beginning and end of each hour; (35) specifies the evolution of the load energy state; and (36) sets the load energy state at the beginning and end of the day to 50% of its maximum capacity (which corresponds to baseline

operation). Since (35) is linear, (33) and (34) ensure that the load energy state is within its limits throughout each hour. Together these constraints ensure that the generator and load dispatch corresponds to the wind power and temperature forecasts. This means that if the forecasts are perfect no reserves are needed. Unless the forecast errors are single sign (i.e., all negative or all positive) the inequality constraints will be redundant with their probabilistic counterparts.

2) Probabilistic Constraints: At *Operating Point 1* generator production and controllable load consumption are

$$P^{new}_{G,t} = P_{G,t} + R_{GS,t} + R^{b}_{GD,t},$$
$$P^{new}_{C,t} = P_{C,t} + R_{LS,t} + R^{b}_{LD,t},$$

where the reserve shifts are given in (8), (9), (16), and (17). The new power injection is

$$P^{new}_{inj,t} = C_G P^{new}_{G,t} + C_W P_{W,t} - C_L(P_{L,t} + P^{new}_{C,t}) \tag{37}$$

and the constraints that must be enforced are

$$-P_l \le AP^{new}_{inj,t} \le P_l, \tag{38}$$
$$\underline{P}_G \le P^{new}_{G,t} \le \overline{P}_G, \tag{39}$$
$$0 \le P^{new}_{C,t} \le \overline{P}_C(T_t), \tag{40}$$
$$-\underline{R}_{GS,t} \le R_{GS,t} \le \overline{R}_{GS,t}, \tag{41}$$
$$-\underline{R}_{LS,t} \le R_{LS,t} \le \overline{R}_{LS,t}, \tag{42}$$
$$-\underline{R}_{GD,t} \le R^{b}_{GD,t} \le \overline{R}_{GD,t}, \tag{43}$$
$$\text{constraints (10), (11), (18), (19),}$$

where (41)-(43) determine the generator secondary reserve capacity, load secondary reserve capacity, and generator redispatch capacity, respectively. Note that load deviations due to redispatch actions (i.e., $R^{b/b_o/w/w_o}_{LD,t}$) only correct load energy state deviations. Therefore, they are not considered reserve actions and are not financially rewarded.

At *Operating Point 2* generator production and controllable load consumption are

$$P^{new}_{G,t} = P_{G,t} + R^{w}_{GD,t} + R^{b}_{GD,t},$$
$$P^{new}_{C,t} = P_{C,t} + R^{w}_{LD,t} + R^{b}_{LD,t},$$

where the reserve shifts are given in (12), (13), (16), and (17). The new power injection is (37) and constraints that must be enforced are

$$\text{constraints (14), (15), (18), (19), (38)} - \text{(40)},$$
$$-\underline{R}_{GD,t} \le R^{w}_{GD,t} + R^{b}_{GD,t} \le \overline{R}_{GD,t}. \tag{44}$$

At *Operating Point 3* generator production and controllable load consumption are

$$P^{new}_{G,t} = P_{G,t} + R_{GS,t} + R^{w_o}_{GD,t} + R^{b_o}_{GD,t},$$
$$P^{new}_{C,t} = P_{C,t} + R_{LS,t} + R^{w_o}_{LD,t} + R^{b_o}_{LD,t},$$

where the reserve shifts are given in (8), (9), (20)–(23). The new power injection is (37) and constraints that must be enforced are

$$\text{constraints (10), (11), (24)} - \text{(27), (38)} - \text{(42)},$$
$$-\underline{R}_{GD,t} \le R^{w_o}_{GD,t} + R^{b_o}_{GD,t} \le \overline{R}_{GD,t}. \tag{45}$$

We also need to ensure that the controllable load energy capacity limits are satisfied. The following constraints are sufficient to ensure that the load energy state remains within its limits within $[t, t+1]$. Specifically, since the energy state dynamics are linear, the energy capacity limits are satisfied within each interval of the hour, if they are satisfied at the end of the first and last interval of the hour, i.e.,

$$0 \le S_t + \big(P_{C,t} + R_{LS,t} - P_B(T_t)\big)\frac{\Delta\tau}{n} \le \overline{S}(T_t), \tag{46}$$
$$0 \le S_t + \Big(P_{C,t} - P_B\Big(T^f_t\Big)\Big)\frac{(n-1)\Delta\tau}{n} + \big(P_{C,t} + R_{LS,t} - P_B(T_t)\big)\frac{\Delta\tau}{n} \le \overline{S}(T_t). \tag{47}$$

For simplicity, define x to be a stacked version of $\{x_t\}_{t=1}^{N_t}$ and let $\delta_t \in \mathbb{R}^{N_W+N_T}$ denote the uncertainty vector in timestep t, where N_W is the number of wind power plants, i.e., $P_{W,t} \in \mathbb{R}^{N_W}$, and N_T is the number of temperature zones, i.e., $T_t \in \mathbb{R}^{N_T}$. We require constraints that are affected by δ_t to be satisfied with probability of at least $1-\varepsilon_t$, where ε_t is the violation level. Then, the optimization problem can be formulated as a quadratic program with multiple chance constraints. For each $t = 2, \ldots, N_t$, the chance constraints can be written compactly as

$$\mathbb{P}(H_t(\delta_t, \delta_{t-1})x + h_t + g_t(\delta_t) \le 0) \ge 1 - \varepsilon_t,$$

where H_t, h_t, and g_t are functions used to split each constraint into terms that have random variables that multiply decision variables, terms that have neither random variables nor decision variables, and terms that have random variables but no decision variables, respectively. For $t = 1$, the chance constraint is similar except that H_1 depends only on δ_1.

IV. Scenario-Based Solution Methodology

We solve the optimization problem using a probabilistically robust optimization method [11], [12] that is a mixture of randomized and robust optimization, and is more computationally tractable than the scenario approach [32]. It does not require assumptions on the probability distributions of the uncertainty and provides guarantees on the probability of constraint satisfaction.

The method includes two steps. In the first step, for each $t = 1, \ldots, N_t$, the scenario approach [32] is used to determine, with a confidence of at least $1-\beta_t$, the minimum volume set that contains at least $1-\varepsilon_t$ probability mass of the uncertainty. Let this set be denoted by Δ_t. To compute this set, the number of scenarios we need to use is given by

$$N_{s,t} \le \frac{1}{\varepsilon_t}\frac{e}{e-1}\left(\ln\frac{1}{\beta_t} + 4(N_W + N_T) - 1\right).$$

In the second step, we use Δ_t to formulate a robust problem where the uncertainty is confined in this set. For each $t = 2, \ldots, N_t$, the chance constraint is replaced by the following robust constraint

$$H_t(\delta_t, \delta_{t-1})x + h_t + g_t(\delta_t) \le 0, \ \ \forall(\delta_t, \delta_{t-1}) \in \Delta_t \times \Delta_{t-1}.$$

For $t = 1$, the constraint is similar except that H_1 depends only on δ_1 and we require the constraint to be satisfied for all $\delta_1 \in \Delta_1$. Following [11], [12], any feasible solution satisfying the robust constraints will be feasible for the chance constraints with a confidence of at least $1 - \beta_t$. To solve the resulting convex problem, standard techniques for robust optimization can be employed [33].

V. Cost Parameter Rules

We next derive cost parameter rules that indicate which reserve resource will be preferred. We base our analysis on a simpler optimization problem and discuss how the results give us intuition for the solution of the full problem.

For simplicity, we consider a cost function that minimizes reserve costs only and we assume symmetric reserve deployment (i.e., $d = \overline{d} = \underline{d}$, where d is any distribution vector), ignore the temperature error, and consider a single hour. Let a scenario $i \in \{1, \ldots, N_v\}$ of the total wind power error be denoted by w_i, where N_v is the number of scenarios that correspond to the vertices of the hyper-rectangular box defining the robust uncertainty set. The reserve capacities $\mathcal{R}$ will be determined by the worst case reserve actions, e.g., $\overline{R}_{GS} = \max_i(-d_{GS}w_i)$. Let Δw denote the difference between the extreme values of w_i, i.e., $\Delta w = \max_i(w_i) - \min_i(w_i)$. Then the simplified optimization problem is

$$\min_{d} \; c_{GS}^T d_{GS}\Delta w + c_{LS}^T d_{LS}\Delta w + c_{GD}^T d_{GD}\Delta w \tag{48}$$

$$\text{s.t.} \; \mathbf{1}^T d_{GS} + \mathbf{1}^T d_{LS} = 1, \tag{49}$$

$$\mathbf{1}^T d_{GD} = 1 + \mathbf{1}^T d_{LS}, \tag{50}$$

$$d_{GS}, d_{LS}, d_{GD} \geq 0. \tag{51}$$

This problem has a trivial solution which schedules secondary reserve capacity from the cheapest generator if $\min(c_{GS}) \leq \min(c_{LS}) + \min(c_{GD})$ and from the cheapest load otherwise. However, in the full problem, additional constraints (e.g., limits on the amount of reserves each resource can contribute, line limits) will generally require us to schedule reserve capacity from multiple generators and loads.

We next derive a stronger cost parameter rule. First, we remove Δw from the cost function since it does not affect the solution, and define $J(d) = c_{GS}^T d_{GS} + c_{LS}^T d_{LS} + c_{GD}^T d_{GD}$. Assume that there exists a $d^{(1)} \in D_1$ where D_1 is the feasibility set of (49)–(51), implying that both generators and loads may provide secondary reserves. Assume also that there exists a $d^{(2)} \in D_2$ where D_2 is the feasibility set of (49)–(51) and an additional constraint $\mathbf{1}^T d_{LS} = 1$, implying that only loads provide secondary reserves. We would like to find c_{GS}, c_{LS}, c_{GD} such that $J(d^{(1)}) \geq J(d^{(2)})$, i.e., the cost of scheduling any generator-based reserves is greater than or equal to scheduling only load-based reserves.

Notice that for every $[d_{GS}^{(1)}, d_{LS}^{(1)}, d_{GD}^{(1)}] \in D_1$ there aways exists $[0, d_{LS}^{(2)}, d_{GD}^{(2)}] \in D_2$ and $d_{LS}^{(*)}, d_{GD}^{(*)}$ such that $d_{LS}^{(1)} = d_{LS}^{(2)} - d_{LS}^{(*)}$ and $d_{GD}^{(1)} = d_{GD}^{(2)} - d_{GD}^{(*)}$. Let α denote the portion of reserves provided by generators, i.e., $\mathbf{1}^T d_{GS}^{(1)} = \alpha$. Then, $\mathbf{1}^T d_{LS}^{(1)} = 1 - \alpha$ and $\mathbf{1}^T d_{GD}^{(1)} = 2 - \alpha$. Also, by definition, $\mathbf{1}^T d_{LS}^{(2)} = 1$ and $\mathbf{1}^T d_{GD}^{(2)} = 2$. Then, $\mathbf{1}^T d_{LS}^{(*)} = \alpha$ and $\mathbf{1}^T d_{GD}^{(*)} = \alpha$. Therefore,

$$\begin{aligned} J\left(d^{(1)}\right) &= c_{GS}^T d_{GS}^{(1)} + c_{LS}^T d_{LS}^{(1)} + c_{GD}^T d_{GD}^{(1)}, \\ &= J\left(d^{(2)}\right) + c_{GS}^T d_{GS}^{(1)} - c_{LS}^T d_{LS}^{(*)} - c_{GD}^T d_{GD}^{(*)}, \end{aligned}$$

and so, if we select the cost parameters such that

$$c_{GS}^T d_{GS}^{(1)} - c_{LS}^T d_{LS}^{(*)} - c_{GD}^T d_{GD}^{(*)} \geq 0, \tag{52}$$

we achieve $J(d^{(1)}) \geq J(d^{(2)})$. Since the cost parameters are positive, (52) holds if

$$\begin{aligned} &\min(c_{GS})\mathbf{1}^T d_{GS}^{(1)} - \max(c_{LS})\mathbf{1}^T d_{LS}^{(*)} - \max(c_{GD})\mathbf{1}^T d_{GD}^{(*)} \geq 0 \\ &\quad \Rightarrow (\min(c_{GS}) - \max(c_{LS}) - \max(c_{GD}))\alpha \geq 0. \end{aligned}$$

Since $\alpha \geq 0$, for any $d^{(1)} \in D_1$ we can construct a $d^{(2)} \in D_2$ such that

$$\begin{aligned} &\min(c_{GS}) - \max(c_{LS}) - \max(c_{GD}) \geq 0 \\ &\quad \Rightarrow \quad J\left(d^{(1)}\right) \geq J\left(d^{(2)}\right). \end{aligned} \tag{53}$$

Similarly, assume that there exists a $d^{(3)} \in D_3$ where D_3 is the feasibility set of (49)–(51) and an additional constraint $\mathbf{1}^T d_{GS} = 1$ (i.e., $\alpha = 1$), implying that only generators provide secondary reserves. We can also show that for any $d^{(1)} \in D_1$

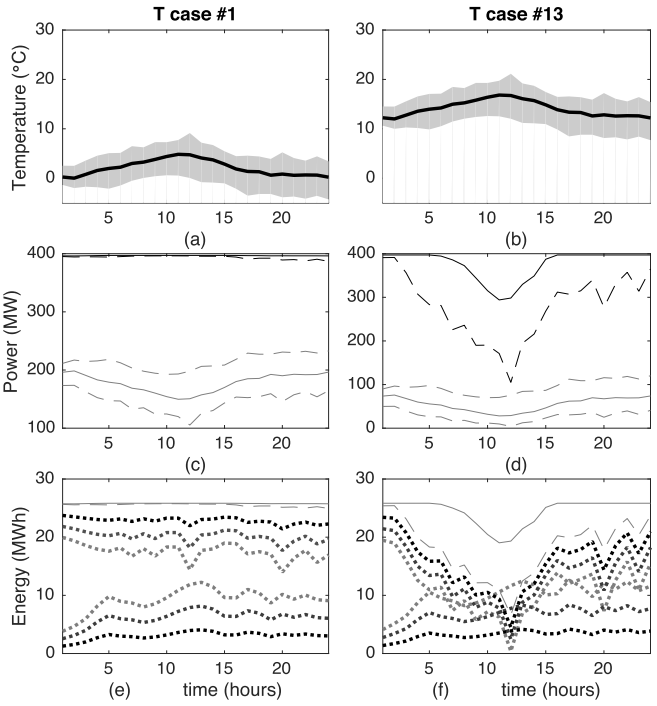

Fig. 3. Influence of temperature forecast profiles on baseline power and capacity limits. (a), (b) *Two temperature forecast profiles*, where the black line shows the temperature forecast and the gray area spans the forecast errors. (c), (d) *Baseline power and power capacity*, where the solid gray line shows the baseline power forecast, the dashed gray lines show the worst-case baseline, the solid black line shows the power capacity limit forecast, and the dashed black line shows the worst-case power capacity limit. (e), (f) *Energy capacity*, where the solid gray line shows the energy capacity limit forecast, the dashed gray line shows the worst-case energy capacity limit, and the dotted lines show the tightening of the energy capacity limits due to baseline errors for $n = 12, 6, 4$, respectively.

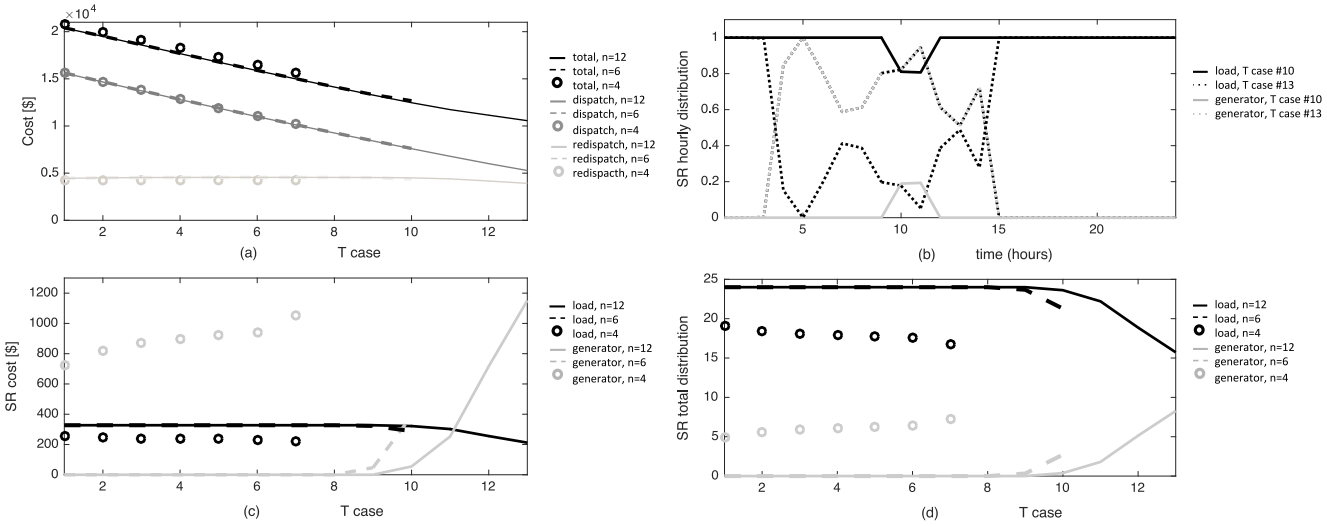

Fig. 4. Costs and secondary reserve (SR) distribution for 13 T cases. (a) Total, dispatch, and redispatch costs. (b) Examples of hourly distribution of the secondary reserves for $n = 12$ and T cases #10 and #13. (c) Secondary reserve costs. (d) Total distribution of secondary reserves.

we can construct a $d^{(3)} \in D_3$ such that

$$\max(c_{GS}) - \min(c_{LS}) - \min(c_{GD}) \leq 0 \quad \Rightarrow \quad J\left(d^{(1)}\right) \geq J\left(d^{(3)}\right). \tag{54}$$

VI. Case Studies

A. Set-Up

We tested the approach on the IEEE 30-bus network using cost/parameter settings from MATPOWER [34]. We modified the network to include 4 wind power plants (i.e., $N_W = 4$) connected to buses 1, 2, 22, and 27 with capacities 10, 10, 20, and 10 MW, respectively. We also increased the line capacity limits by 50%. We defined 13 temperature forecast profiles (referred to as "T cases"), where the first corresponds to Fig. 3 (a), the last to Fig. 3 (b), and intermediary cases shift all temperatures by 1° C. We used load profiles from NREL [35] and modeled all loads as partially controllable. Specifically, we assumed two-thirds of each load in the first hour of the day corresponding to T case #12 is controllable. Then, for the remainder of the day, the portion of controllable load is determined by the temperature. We assumed all loads are affected by the same temperature, i.e., $N_T = 1$, and symmetric reserve deployment, though neither assumption is a requirement of the method. We set the reserve costs to ensure generators reap profit from providing reserves and loads are generally preferred. Specifically, we set each generator's secondary reserve costs to be 5 times its linear energy cost and redispatch costs to be equal to its linear energy costs, and we set each load's secondary reserve costs to be 0.5 $/MW. Wind power and temperature forecast error scenarios were generated using real data and the Markov Chain Monte Carlo mechanism described in [36]. Specifically, we used forecasted and actual hourly wind power data from Germany and forecasted and actual hourly temperature data from eleven weather stations in Switzerland to train a transition probability matrix that we then used to generate the scenarios. We set $\varepsilon_t = 10\%$ and $\beta_t = 10^{-4} \quad \forall t = 1, \ldots, N_t$ and so we needed 447 uncertainty scenarios. We evaluated the empirical violation probability using 10, 000 independent scenarios. All optimization problems were solved using the solver MOSEK via the MATLAB interface CVX. Computational times are presented in Part II and on the order of tens of seconds for the IEEE 30-bus network.

B. Results

Fig. 3 shows how the baseline power and energy capacity limits are influenced by the forecast profiles and their errors, and by the redispatch interval (i.e., 5, 10, or 15 minutes, corresponding to $n = 12, 6, 4$, respectively). To ensure a feasible dispatch, the controllable load power consumption set points should lie between the dashed black line and zero in (c), (d), and the load energy state trajectory should lie between the dotted lines corresponding to the redispatch interval in (e), (f). Lower temperatures (left) lead to larger forecasted reserve capacities (since more electric space heaters are available) and, subsequently, larger feasible regions. The number of redispatch intervals influences the feasible region of the load energy state trajectory, specifically, the more often the system is redispatched the better it can manage forecast error. In (f), for $n = 6, 4$, there is no feasible load energy state trajectory.

Fig. 4 shows the costs and secondary reserve distributions for all T cases. The cost parameters satisfy (53). As shown in (a), the total operational costs decrease with temperature since the controllable loads (heaters) need to consume less power. However, as shown in (c), the secondary reserve costs increase with temperature since loads provide less reserves, as shown also in (d), in which we have plotted the sum of the loads' and generators' distribution vectors over 24 hours (a value of 24 corresponds to all secondary reserves being provided by loads). As shown in (b), generators have to provide more reserves in the middle of the day when temperatures are higher.

The worst-case empirical violation probability (over all T cases and redispatch intervals) is 1.86% as compared to the

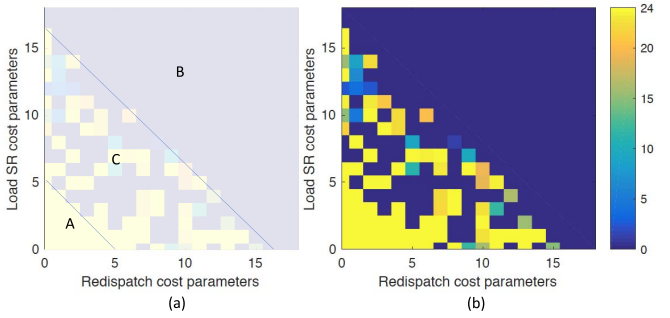

Fig. 5. Allocation of secondary reserves as a function of load secondary reserve costs and redispatch costs. Yellow (dark blue) corresponds to cases in which loads (generators) provide all secondary reserves. (a) Area A corresponds to (53), Area B corresponds to (54), and Area C corresponds to neither. (b) Results of each optimization run.

desired probability of 10%. This demonstrates the validity of the scenario-based method but also its conservatism, which is inherent since we are using a robust reformulation [11], [12].

Fig. 5 shows the allocation of secondary reserves as a function of the load secondary reserve costs and the redispatch costs, allowing us to visualize the cost rules (53) and (54) for $n = 12$ and T case #2. To create the plot, we fixed c_{GS} (each entry taking a value from 5 to 16.25 \$/MW) and drew random values for c_{LS} and c_{GD} that i) satisfied (53), corresponding to set A; ii) satisfied (54), corresponding to set B; or iii) neither, corresponding to set C. For each set of cost parameters, we solved the problem and calculated the total distribution of secondary reserves to loads and generators. Cost parameter vectors were mapped to the axes as follows: each value of the axis up to 5 corresponds to the maximum entry of the vector (i.e., the highest cost), each value beyond 16.25 corresponds to the minimum entry of the vector (i.e., the lowest cost), and each value in between corresponds to either the maximum or minimum value of the vector. Based on the cost rules, we would expect loads to provide all reserves for $5 - y - x \geq 0$ (area marked with an A) and generators to provide all reserves for $16.25 - y - x \leq 0$ (area marked with a B), which is consistent with the plot. Between the two lines (area marked with a C), we can not predict the outcome based on the cost rules. Note that the rules only apply when there is sufficient load flexibility; otherwise the generators will provide reserves.

VII. Concluding Remarks

We formulated a multi-period CC-OPF to schedule power production and both generator and load-based reserve capacities. We modeled controllable loads as thermal energy storage units and designed a redispatch mechanism to manage their energy states to reduce uncertainty propagation throughout the time horizon. We considered uncertainty in both wind power and outdoor temperature forecasts, where the latter affects the available capacity from the controllable loads. We solved the CC-OPF problem using probabilistically robust optimization. Relations between the reserve cost parameters, which determine when load-based reserves will be preferred over generator reserves, were derived.

References

[1] D. S. Callaway and I. A. Hiskens, "Achieving controllability of electric loads," *Proc. IEEE*, vol. 99, no. 1, pp. 184–199, Jan. 2011.

[2] J. L. Mathieu, S. Koch, and D. S. Callaway, "State estimation and control of electric loads to manage real-time energy imbalance," *IEEE Trans. Power Syst.*, vol. 28, no. 1, pp. 430–440, Feb. 2013.

[3] S. P. Meyn, P. Barooah, A. Busić, Y. Chen, and J. Ehren, "Ancillary service to the grid using intelligent deferrable loads," *IEEE Trans. Autom. Control*, vol. 60, no. 11, pp. 2847–2862, Nov. 2015.

[4] A. Khodaei, M. Shahidehpour, and S. Bahramirad, "SCUC with hourly demand response considering intertemporal load characteristics," *IEEE Trans. Smart Grid*, vol. 2, no. 3, pp. 564–571, Sep. 2011.

[5] A. Papavasiliou and S. S. Oren, "Large-scale integration of deferrable demand and renewable energy sources," *IEEE Trans. Power Syst.*, vol. 29, no. 1, pp. 489–499, Jan. 2014.

[6] A. Papavasiliou, S. S. Oren, and R. P. O'Neill, "Reserve requirements for wind power integration: A scenario-based stochastic programming framework," *IEEE Trans. Power Syst.*, vol. 26, no. 4, pp. 2197–2206, Nov. 2011.

[7] H. Zhang and P. Li, "Chance constrained programming for optimal power flow under uncertainty," *IEEE Trans. Power Syst.*, vol. 26, no. 4, pp. 2417–2424, Nov. 2011.

[8] M. Vrakopoulou, K. Margellos, J. Lygeros, and G. Andersson, "Probabilistic guarantees for the N-1 security of systems with wind power generation," in *Proc. Int. Conf. Probabilistic Methods Appl. Power Syst.*, 2012, pp. 59–73.

[9] M. Vrakopoulou, K. Margellos, J. Lygeros, and G. Andersson, "A probabilistic framework for reserve scheduling and N-1 security assessment of systems with high wind power penetration," *IEEE Trans. Power Syst.*, vol. 28, no. 4, pp. 3885–3896, Nov. 2013.

[10] J. L. Mathieu, M. G. Vayá, and G. Andersson, "Uncertainty in the flexibility of aggregations of demand response resources," in *Proc. Annu. Meeting IEEE Ind. Electron. Soc.*, Vienna, Austria, 2013, pp. 8052–8057.

[11] K. Margellos, P. Goulart, and J. Lygeros, "On the road between robust optimization and the scenario approach for chance constrained optimization problems," *IEEE Trans. Autom. Control*, vol. 59, no. 8, pp. 2258–2263, Aug. 2014.

[12] X. Zhang, K. Margellos, P. Goulart, and J. Lygeros, "Stochastic model predictive control using a combination of randomized and robust optimization," in *Proc. IEEE Conf. Decis. Control*, Florence, Italy, 2013, pp. 7740–7745.

[13] D. Bienstock, M. Chertkov, and S. Harnett, "Chance-constrained optimal power flow: Risk-aware network control under uncertainty," *SIAM Rev.*, vol. 56, no. 3, pp. 461–495, 2014.

[14] L. Roald, F. Oldewurtel, T. Krause, and G. Andersson, "Analytical reformulation of security constrained optimal power flow with probabilistic constraints," in *Proc. IEEE PowerTech*, Grenoble, France, 2013, pp. 1–6.

[15] Y. Zhang, S. Shen, and J. L. Mathieu, "Distributionally robust chance-constrained optimal power flow with uncertain renewables and uncertain reserves provided by loads," *IEEE Trans. Power Syst.*, vol. 32, no. 2, pp. 1378–1388, Mar. 2017.

[16] M. Vrakopoulou, M. Katsampani, K. Margellos, J. Lygeros, and G. Andersson, "Probabilistic security-constrained AC optimal power flow," in *Proc. IEEE PowerTech Conf.*, Grenoble, France, 2013, pp. 1–6.

[17] E. Dall'Anese, K. Baker, and T. Summers, "Chance-constrained AC optimal power flow for distribution systems with renewables," *IEEE Trans. Power Syst.*, vol. 32, no. 5, pp. 3427–3438, Sep. 2017.

[18] M. Vrakopoulou, J. Mathieu, and G. Andersson, "Stochastic optimal power flow with uncertain reserves from demand response," in *Proc. Hawaii Int. Conf. Syst. Sci.*, Waikoloa, HI, USA, 2014, pp. 2353–2362.

[19] B. Li and J. L. Mathieu, "Analytical reformulation of chance-constrained optimal power flow with uncertain load control," in *Proc. IEEE PowerTech*, Eindhoven, The Netherlands, 2015, pp. 1–6.

[20] J. L. Mathieu, M. Kamgarpour, J. Lygeros, G. Andersson, and D. S. Callaway, "Arbitraging intraday wholesale energy market prices with aggregations of thermostatic loads," *IEEE Trans. Power Syst.*, vol. 30, no. 2, pp. 763–772, Mar. 2015.

[21] C.-Y. Chong and A. Debs, "Statistical synthesis of power system functional load models," in *Proc. IEEE Conf. Decis. Control*, Fort Lauderdale, FL, USA, 1979, pp. 264–269.

[22] S. Ihara and F. C. Schweppe, "Physically based modeling of cold load pickup," *IEEE Trans. Power App. Syst.*, vol. PAS-100, no. 9, pp. 4142–4150, Sep. 1981.

[23] D. S. Callaway, "Tapping the energy storage potential in electric loads to deliver load following and regulation, with application to wind energy," *Energy Convers. Manag.*, vol. 50, no. 5, pp. 1389–1400, 2009.
[24] J. L. Mathieu, M. E. H. Dyson, and D. S. Callaway, "Resource and revenue potential of California residential load participation in ancillary services," *Energy Policy*, vol. 80, pp. 76–87, May 2015.
[25] J. Liu, S. Li, W. Zhang, J. L. Mathieu, and G. Rizzoni, "Planning and control of electric vehicles using dynamic energy capacity models," in *Proc. IEEE Conf. Decis. Control (CDC)*, Florence, Italy, Dec. 2013, pp. 379–384.
[26] H. Hao, B. M. Sanandaji, K. Poolla, and T. L. Vincent, "Aggregate flexibility of thermostatically controlled loads," *IEEE Trans. Power Syst.*, vol. 30, no. 1, pp. 189–198, Jan. 2015.
[27] D. Madjidian, M. Roozbehani, and M. A. Dahleh, "Battery capacity of deferrable energy demand," in *Proc. IEEE Conf. Decis. Control*, Las Vegas, NV, USA, 2016, pp. 4220–4225.
[28] D. Madjidian, M. Roozbehani, and M. A. Dahleh, "Emulating batteries with deferrable energy demand," in *Proc. Amer. Control Conf.*, Seattle, WA, USA, 2017, pp. 2106–2111.
[29] M. Bucksteeg, L. Niesen, and C. Weber, "Impacts of dynamic probabilistic reserve sizing techniques on reserve requirements and system costs," *IEEE Trans. Sustain. Energy*, vol. 7, no. 4, pp. 1408–1420, Oct. 2016.
[30] M. Vrakopoulou, K. Margellos, J. Lygeros, and G. Andersson, "A probabilistic framework for security constrained reserve scheduling of networks with wind power generation," in *Proc. IEEE EnergyCon*, Florence, Italy, 2012, pp. 452–457.
[31] *Regulation Energy Management Draft Final Proposal*, California ISO, Folsom, CA, USA, Jan. 2011. [Online]. Available: http://www.caiso.com/Documents/RevisedDraftFinalProposal-RegulationEnergyManagement-Jan13_2011.pdf
[32] M. C. Campi, G. Calafiore, and M. Prandini, "The scenario approach for systems and control design," *Annu. Rev. Control*, vol. 33, no. 2, pp. 149–157, 2009.
[33] D. Bertsimas and M. Sim, "Tractable approximations to robust conic optimization problems," *Math. Program. B*, vol. 107, nos. 1–2, pp. 5–36, 2006.
[34] R. D. Zimmerman, C. E. Murillo-Sanchez, and R. J. Thomas, "MATPOWER: Steady-state operations, planning, and analysis tools for power systems research and education," *IEEE Trans. Power Syst.*, vol. 26, no. 1, pp. 12–19, Feb. 2011.
[35] A. Hoke, R. Butler, J. Hambrick, and B. Kroposki, "Steady-state analysis of maximum photovoltaic penetration levels on typical distribution feeders," *IEEE Trans. Sustain. Energy*, vol. 4, no. 2, pp. 350–357, Apr. 2013.
[36] G. Papaefthymiou and B. Klockl, "MCMC for wind power simulation," *IEEE Trans. Energy Convers.*, vol. 23, no. 1, pp. 234–240, Mar. 2008.

Maria Vrakopoulou (S'09–M'14) received the Diploma degree in electrical and computer engineering from the University of Patras, Greece, in 2008 and the Ph.D. degree from the Department of Electrical Engineering and Information Technology, ETH Zurich, Switzerland, in 2013. She was a Post-Doctoral Fellow with the University of Michigan, Ann Arbor, MI, USA, and the University of California at Berkeley, Berkeley, CA, USA. Since 2017, she has been a Marie Curie Post-Doctoral Fellow with the Automatic Control Laboratory, Department of Electrical Engineering and Information Technology, ETH Zurich. Her research interests concentrate on the optimization and analysis of planning problems for power systems under uncertainty.

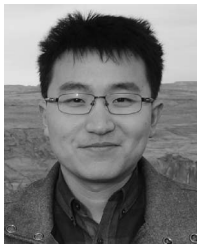

Bowen Li (S'12) received the B.S. degree in mechanical engineering from Shanghai Jiao Tong University, Shanghai, China, and the B.S. and M.S. degrees in electrical engineering from the University of Michigan, Ann Arbor, MI, USA, in 2013 and 2015, respectively, where he is currently pursuing the Ph.D. degree. His research interests include developing and evaluating models and formulations used in stochastic optimal power flow problems with uncertainties from renewable resources and demand response.

Johanna L. Mathieu (S'10–M'12) received the B.S. degree in ocean engineering from the Massachusetts Institute of Technology, Cambridge, MA, USA, in 2004 and the M.S. and Ph.D. degrees in mechanical engineering from the University of California at Berkeley, Berkeley, USA, in 2008 and 2012, respectively. She was a Post-Doctoral Researcher with the Swiss Federal Institute of Technology (ETH) Zurich, Switzerland. She is an Assistant Professor with the Department of Electrical Engineering and Computer Science, University of Michigan, Ann Arbor, MI, USA. Her research interests include modeling, estimation, control, and optimization of distributed energy resources.